HHS Public Access

Author manuscript

Nanotechnology. Author manuscript; available in PMC 2017 August 18.

Published in final edited form as:

Nanotechnology. 2014 January 10; 25(1): 014009. doi:10.1088/0957-4484/25/1/014009.

Cardiac Tissue Engineering in Magnetically Actuated Scaffolds

Yulia Sapir[1], **Boris Polyak**[2,3,*], and **Smadar Cohen**[1,4,5,*]

[1]The Avram and Stella Goldstein-Goren Department of Biotechnology Engineering, Ben-Gurion University of the Negev, Beer-Sheva 84105, Israel

[2]Department of Surgery, Drexel University College of Medicine, Philadelphia PA 19102, USA

[3]Department of Pharmacology and Physiology, Drexel University, Philadelphia, PA 19102, USA

[4]Center for Regenerative Medicine and Stem Cell (RMSC) Research, Ben-Gurion University of the Negev, Beer-Sheva 84105, Israel

[5]Ilse Katz Institute for Nanoscale Science and Technology, Ben-Gurion University of the Negev, Beer- Sheva 84105, Israel

Abstract

Cardiac tissue engineering offers new possibilities for the functional and structural restoration of damaged or lost heart tissue by applying cardiac patches created *in vitro*. Engineering such functional cardiac patches is a complex mission, involving material design on the nano- and micro-scale as well as the application of biological cues and stimulation patterns to promote cell survival and organization into a functional cardiac tissue. Herein, we present a novel strategy for creating a functional cardiac patch by combining the use of a macroporous alginate scaffold impregnated with magnetically responsive nanoparticles (MNPs) and the application of external magnetic stimulation. Neonatal rat cardiac cells seeded within the magnetically-responsive scaffolds and stimulated by an alternating magnetic field of 5Hz developed into matured myocardial tissue characterized by anisotropically organized striated cardiac fibers, which preserved its features for longer times than nonstimulated constructs. A greater activation of AKT phosphorylation in cardiac cell constructs after applying a short-term (20 min) external magnetic field indicated the efficacy of magnetic stimulation to actuate at a distance and provided a possible mechanism for its action. Our results point to a synergistic effect of magnetic field stimulation together with nanoparticulate features of the scaffold surface as providing the regenerating environment for cardiac cells driving their organization into functionally mature tissue.

Introduction

Cardiac tissue engineering (CTE) aims to create contractile heart muscle tissues, able to replace missing (due to congenital heart defect) or dysfunctional parts of the heart (due to myocardial infarction), thus leading to cardiac repair (Ruvinov et al., 2012). Currently, a leading CTE strategy is the *in vitro* engineering of a cardiac patch by seeding cardiomyocytes (CMs) as well as nonmyocyte cells in a scaffold, followed by the application

*To whom correspondence should be addressed: bpolyak@drexelmed.edu; scohen@bgu.ac.il.

of inductive biological and physical cues to promote tissue maturation and function (Radisic et al., 2004, Shachar et al., 2012, Dvir et al., 2007, Barash et al., 2010, Zimmermann et al., 2000, Heidi Au et al., 2009, Gerecht-Nir et al., 2006, Dvir et al., 2009).

In recent years, it has become clear that the nanoscale chemical and structural features of a scaffold play a crucial role in tissue engineering and can affect cell re-organization and tissue development. The nanomaterials can be structured as nanofibers (Zhang et al., 2011a, Orlova et al., 2011), be integrated with specific recognition nanosites (Shachar et al., Sapir et al., 2011), or be bulk materials impregnated with nanoparticles (You et al., 2011, Dvir et al., 2011). For example, we have shown that integrating two different cell signaling peptides into an inert macroporous alginate scaffold induces the formation of a more mature cardiac tissue, *in vitro* (Sapir et al., 2011).

Another critical parameter in cardiac tissue engineering is the application of physical stimulation during cultivation. Most works focus on electrical stimulation or mechanical stretching and compression of the cardiac patch. These approaches, while achieving a significant improvement in promoting tissue formation, are efficient only when employed in a close proximity to the cells in the engineered patch. Additionally, these methods are limited to only provide stimulation *in vitro*.

Our group explores magnetic stimulation to promote cell arrangement and tissue formation in a macroporous alginate scaffold impregnated with magnetic nanoparticles (MNPs). Such a strategy enables actuation at a distance on the nanoscale and cell level. The desired process can be actuated within a target cell by magnetically responsive materials due to its coupling to a magnetic field, regardless of whether there are intervening structures such as tissues. Furthermore, the magnetic field can penetrate deep into tissues, reaching a single cell and acting directly on its organelles; unlike the electric field, which is shielded by the membrane potential. Stress parameters can also be varied dynamically simply by varying the properties (e.g. strength, frequency) of the applied field. Polymer-based nanocomposites loaded with magnetic particles have already been demonstrated as potential candidates for pulsatile drug delivery and soft actuator applications (Edelman et al., 1984, Liu et al., 2006, Zhao et al.). In our previous work (Sapir et al., 2012), we have shown that magnetite-impregnated alginate scaffolds in combination with externally applied alternating field created a stimulating microenvironment suitable for promoting organization of endothelial cells into capillary-like structures *in vitro*.

In the present paper, we explore whether impregnation of alginate scaffolds with magnetically responsive nanoparticles (MNP) and subsequent exposure to an alternating magnetic field at a physiologically relevant frequency (5Hz) would promote the formation of a functional myocardial tissue. The current work is our next step in understanding of how to precisely control cellular organization to form tissue engineered constructs. This, together with additional molecular signals, could lead to a creation of functional myocardial tissue ready for transplantation.

Materials and Methods

Materials

Sodium alginate (LVG, 100 kDa, >65% guluronic acid) was obtained from NovaMatrix FMC Biopolymers (Drammen, Norway). Ferric chloride hexahydrate, ferrous chloride tetrahydrate, D-gluconic acid, hemicalcium salt and sodium hydroxide were obtained from Sigma-Aldrich (St. Louis, MO, USA and Rehovot, Israel). Tissue culture reagents were from Biological Industries (Kibbutz Beit-HaEmek, Israel), MediaTech (Manassas, VA) and Gemini Bio-Products (West Sacramento, CA). Alginate was modified with functional peptides RGD and heparin binding peptide (HBP) as was previously described (Sapir et al., 2011).

Magnetite preparation

The magnetite was obtained by alkaline precipitation of ferrous and ferric chloride (the Massart method. Briefly, four batches of magnetite obtained from ferric chloride hexahydrate and ferrous chloride tetrahydrate (at a molar ratio 2:1, weighing 520 mg and 192 mg, respectively dissolved in 6.2 ml of doubly deionized water) by alkaline precipitation with aqueous sodium hydroxide (a 3.8 ml of 2N sodium hydroxide) were magnetically separated and washed twice with 5 ml of water (Chorny et al., 2007, Johnson et al.). All four batches of magnetite were combined for a total of 890 mg and dispersed in 11 ml of 1.2% (w/v) alginate solution. The magnetite suspension in alginate was heated on a water bath (90°C) for 20 min with periodic mixing. Then the suspension was cooled down to room temperature and sonicated at a maximum power for 5 min (550 Sonic Dismembrator, Fisher Scientific, USA) keeping the tube chilled on ice-water bath. The heating and sonication cycles were repeated twice resulting in a stable ferrofluid with a final magnetite concentration of 8% (v/w) magnetite stabilized alginate. Magnetite nanoparticles obtained by the Massart method (Massart, 1981) usually range between 5 and 20 nm in diameter. These particles are not uniform (MacDonald et al., 2010)and tend to aggregate due to strong surface forces and high surface area. Therefore, depending on application the magnetite crystals are usually stabilized with various amphiphilic molecules (Horak et al., 2007). Because our scaffold is comprised of alginate, we stabilized magnetite crystals with sodium alginate to allow good blending between the polysaccharide matrix and magnetite particles. After stabilization of magnetite particles with alginate we obtained magnetite aggregates of a submicron size ranging at 416–776 nm with a polydispersity index of 0.225 (Sapir et al., 2012). Nonetheless, visually the alginate-stabilized ferro-fluid appeared to be homogeneous and was easily miscible with alginate, resulting in uniform distribution of MNP aggregates in alginate solution and in the fabricated scaffold.

Fabrication of macroporous magnetic alginate scaffolds (MNP-scaffolds)

Macroporous scaffolds, with a diameter of 5 mm and 2 mm thickness, were fabricated by a freeze-dry technique (Shapiro and Cohen, 1997). In brief, the alginate was dissolved in DDW to obtain a 1.2% (w/v) solution, and then cross-linked by adding D-gluconic acid, hemicalcium salt (1.22% (w/v)), while stirring the mixture for achieving uniform cross-linking of the alginate. Magnetically responsive alginate scaffolds were fabricated using the same method, from a mixture of alginate (LVG) stabilized ferrofluid and alginate to obtain

1.2% (w/v) and 1.0% (w/v) final concentration of magnetite and alginate post-crosslinking respectively. The cross-linked alginate solution was poured into 96-well plates (100 μL/well), chilled to 2–8°C overnight, frozen at -20°C for 24 h, and lyophilized. Scaffold sterilization was achieved by exposure to UV light. Magnetically responsive scaffolds exhibited a near superparamagnetic behavior showing a slight hysteresis due to particle aggregation at a submicron scale (Sapir et al., 2012).

SEM characterization of MNP-scaffolds

The MNP scaffolds were characterized by Zeiss Supra VP-50 field emission scanning electron microscopy (SEM) using the secondary-electron in-lens detector (at 2.5 kV accelerating voltage). A low voltage was used to image the MNP scaffolds in SEM in order to minimize the effects of charge accumulation. Before imaging, the samples were sputter-coated with carbon for 15 sec using a Cressington 208 high vacuum carbon coater to improve sample's conductivity.

Cell culture

The study was performed with the approval and according to the guidelines of the Institutional Animal Care and Use Committee of the Ben-Gurion University, Israel and Drexel University College of Medicine, USA. Cardiac cells were isolated from the ventricles of 1–3-day old neonatal Sprague-Dawley rats using 6–7 cycles (30 min each) of enzyme digestion with collagenase type II (95 U/mL; Worthington, Lakewood, NJ) and pancreatin (0.6 mg/mL; Sigma) followed by 30 minutes preplating. The cell pools were suspended in culture medium, composed of M-199 supplemented with 0.6 mM $CuSO_4 5H_2O$, 0.5 mM$ZnSO_4 \cdot 7H_2O$, 500 U/mL Penicillin and 100 mg/mL streptomycin (i.e., culture medium) and 5% (v/v) FBS (Dar et al., 2002). The isolated cells consisted of 50 ± 5% cardiomyocytes (Shachar et al., 2011). The cardiac cells were seeded at an initial cell density of 6.4 $\times 10^7/cm^3$ by adding15 mL of the suspended cells onto the scaffolds, placed in 96-well plates, followed by 2-min centrifugation (800 rpm, 4°C) and a short (1 h) incubation (37 °C, 5% CO_2) in 200 μL of culture medium. The cell constructs were then transferred to 6-well plates supplemented with 3 mL of culture medium and incubated under standard conditions.

For the scaffold adhesion studies cardiac fibroblasts collected during the preplating steps were purified by cultivation on cell culture flasks (275 cm^2) in culture medium up to passage 3, then removed from the flasks by 0.25% trypsin/EDTA and counted using trypan blue exclusion assay. The cardiac fibroblasts were seeded at initial density of 0.7×10^7 cell/cm^3 by adding 15 μL of the suspended cells onto the scaffold, placed in 96-well plates, followed by 2-min centrifugation (800 rpm, 4°C) and incubation in 200 μL of culture medium.

Magnetic stimulation setup

Four 60 mm cell culture petri dishes containing 8 scaffolds each were placed in a 45 mm gap between two Helmholtz coils (HHS 5201–98, Schwarzbeck Mess-Elektronik, Schönau, Germany). An AC magnetic field of 10–15 Gauss was produced by passing an electrical current through serially connected coils at frequency 5 Hz. An electrical current of 1.37 A was generated by an OR-X 325 DDS function generator (Rehovot, Israel) and amplified by

AE Techtron 7224 Amplifier (IN, USA). Magnetic-field strength was calibrated by hand-held Lakeshore 410 magnetometer (Lake Shore Cryotronics, Inc., Westerville, OH, USA).

Cell viability and DNA content

Cell viability was evaluated by AlamarBlue™ assay (AbD Seroteck, Kidlington, UK) (Fields and Lancaster, 1993). The constructs (n=3–5) were transferred into new wells and incubated with 1 mL of 10% AlamarBlue™ working solution in DMEM medium with no additives for 2 h. Aliquots of AlamarBlue™ containing medium (300 μL) were placed in a 96-well plate and the fluorescence was measured at an excitation wavelength of 540 nm and emission wavelength of 590 nm using a plate reader Synergy™ 4 (BioTek, USA). Medium-wetted cell-free scaffolds were subjected to the same processes for use as control.

DNA content was analyzed using Quant-iT™ PicoGreen® dsDNA reagent (Molecular probes, Invitrogen, CA, USA) (Singer et al., 1997). The constructs (n=2–3) were dissolved in 200 μL sodium citrate (4% (w/v) in PBS) to free the cells followed by centrifugation (6,000 rpm, 10 min). The cell pellet was suspended in 100 μL lysis buffer (SDS 0.02 % (v/v) in sodium citrate (0.015 M-saline, pH 7) and incubated for 1 h at 37° C. Then, 100 μL of Quant-iT™ PicoGreen® dsDNA assay solution (1:200) was added, followed by 10-min incubation. Aliquots (200 μL) were placed in a 96-well plate and the fluorescence was measured at excitation wavelength of 480 nm and emission wavelength of 520 nm using a plate reader. Medium-wetted cell-free scaffolds were subjected to the same processes for use as control.

Immunostaining and confocal imaging

For immunofluorescence and confocal imaging, the cell constructs were fixed in warm methanol-free formaldehyde (4% in DMEM, (v/v)) for 7 min (Thermo-Fisher Scientific Inc., USA), washed twice in DMEM buffer ($CaCh_2$•$2H_20$ (1.8mM), KCl (5.36mM), $MgSO_4$•$7H_2O$ (0.81mM), NaCl (0.1M), $NHCO_3$ (0.44mM), NaH_2PO_4 (0.9mM)), at pH 7.4, and permeabilized using Triton-X 100 (0.2% (v/v) in DMEM) for 10 min. The constructs were washed 3 times, blocked for 1h at room temperature in DMEM containing 5% BSA (Millipore, Bedford, US) and then washed. The samples were incubated overnight with primary antibodies to detect alpha-actinin (1:450; clone EA-53, Sigma) or vinculin (1:400, Abcam, USA) followed for 4 h incubation with goat anti-mouse Alexa 488 antibody (1:500) and Alexa-Fluor 546-conjugated phalloidin (1:300), which stain F-actin for cell visualization (Molecular Probes, Invitrogen, USA). For nuclei detection, the cells were incubated for 5 min with DAPI reagent (1:30,000; Molecular Probes). Imaging of the cell constructs was performed with an Olympus Fluoview FV1000 laser scanning confocal microscope.

Protein analysis by western blotting

Cell constructs were dissolved in sodium citrate buffer (4% (w/v), pH7.4) to free the cells. The mixture was centrifuged, and the cell pellets suspended in RIPA lysis buffer (Thermo-Fisher Scientific Inc., USA) supplemented with complete protease inhibitor (Roche, Indianapolis, US), then centrifuged. The total extracted protein was measured using BCA reagent assay (Thermo-Fisher Scientific Inc., USA). Equal amounts of the samples were size-fractionated by10% (w/v) sodium dodecyl sulfate polyacrylamide gel electrophoresis

(SDS-PAGE) then electrotransferred for 1 h at 100V to nitrocellulose membranes (BioRad) and blocked in 5% BSA or 5% milk solutions according to the antibody manufacturer instructions. Membranes were probed using antibodies against AKT (1:1,000, Cell Signaling Technologies, Beverly, MA), phospho-AKT (1:1,000, Cell Signaling Technologies, Beverly, MA), p38 (1:1000, Cell Signaling Technologies, Beverly, MA), phospho-p38 (1:1,000, Cell Signaling Technologies, Beverly, MA), cardiac Troponin-T (1:1,000, Abcam, Cambridge, MA), Connexin-43 (1:1,000, Cell Signaling Technologies, Beverly, MA), vimentin (1:5,000, Abcam, Cambridge, MA), PCNA (1:2,000, Sigma-Aldrich, St. Louis, MO) and GAPDH (1:20,000, Sigma-Aldrich, St. Louis, MO), followed by incubation with anti-rabbit/mouse HRP-conjugated or fluorescent (680 nm and 800 nm) secondary antibodies. The membranes probed with HRP-conjugated antibodies were developed using the standard enhanced chemiluminescence (ECL) procedure (Amersham, GE Healthcare, Buckinghamshire, UK). The signal was detected using Fujifilm LAS-4000 imager (Fujifilm UK Ltd, Bedford, UK). The fluorescent labeled membranes were visualized on an Odyssey near-infrared imager model 9201-01 (LI-COR, Lincoln, NE). Densitometry analysis was carried out using ImageJ software.

Statistics

Statistical analysis was performed with GraphPad Prism version 5.03 for Windows (GraphPad Software, San Diego, CA). All variables are expressed as mean±SEM from at least 3 independent experiments. To test the hypothesis whether there were changes in various parameters over time among the experimental groups, a general linear 2-way ANOVA model was used. The model included the effects of treatment, time and treatment-by time of interaction. The Bonferroni's correction was used to assess the significance of predefined comparisons at specific time points. To test the hypothesis whether there were changes between two experimental groups, a t-test was used. $P<0.05$ was considered statistically significant.

Results

Cell adhesion to MNP-impregnated scaffold

Cell adhesion and spreading in the macroporous alginate scaffolds is mediated *via* cell interactions with two matrix-bound adhesive peptides: RGD and heparin binding peptide (HBP), representing different signaling in ECM-cell interactions. We have recently shown that the cardiac tissue developed in the HBP/RGD-attached scaffolds provides the best features of a functional muscle tissue with isotropic myofiber arrangement (Sapir et al., 2011).

In the present study, the scaffolds were impregnated with MNPs to obtain magnetically-responsive scaffolds. Impregnation of MNPs into scaffold walls had no measurable effect on the macropore structure of the scaffolds (71±11 μm, with 98.83% extent of porosity), but did affect their surface topography, as shown by scanning electron micrographs (SEM) (Figure 1). As seen, the MNPs are distributed throughout the entire matrix wall, presenting rough surface topography. MNPs not associated with scaffold's walls were not observed, indicating

on good particle interaction with their stabilizing agent alginate and formation of a uniform composite material.

We examined whether MNP impregnation within the HBP/RGD alginate scaffold wall affects cell adhesion and spreading. Cardiac fibroblasts (CFs) were seeded into the scaffolds at different cultivation times, the constructs were assessed by confocal fluorescent microscope after staining the cells for the cytoskeleton microfilament F-actin (red), and for the focal adhesion protein, vinculin (green) (Figure 2(A)). At 1 h post seeding, the cells had already adhered to the matrix and a few of them started to spread over the matrix (arrows). Spreading of the cells over the matrix was much pronounced at 3 h post seeding and after 24 h, all cells showed a full spread morphology, while interacting with each other.

Effects of short-term magnetic stimulation on cell signaling

To verify that the alternating magnetic field affects the cardiac cells cultivated within the MNP-impregnated scaffolds, we analyzed the activation of AKT and p38, proteins associated with pro-survival (Cardone et al., 1998, Biggs et al., 1999, Brunet et al., 1999) and pro-apoptotic (Wada and Penninger, 2004, Ma et al., 1999) pathways in these cells, respectively. The activation of these pathways has been demonstrated in cardiac cells following the application of various chemical and mechanical cell stimulations (Chen et al., 2001, Dvir et al., 2007, Takahashi et al., 1999), but it has never been examined in three-dimensional (3-D) cell cultures upon exposure of the cell constructs to external magnetic field.

Freshly isolated neonatal cardiac cells, a mixture of cardiomyocytes (CMs) and cardiofibroblasts (CFs), were seeded within MNP-impregnated scaffolds and were allowed to adhere to the matrix for 72 h. The constructs were then exposed to an externally applied alternating magnetic field of 10–15 Oe, at a frequency of 5 Hz for 20 min. Control constructs were cultivated without exposure to a magnetic field. Figure 2(B) reveals that the short-term stimulation of the cardiac cells in MNP-impregnated scaffold by alternating magnetic field at 5Hz induced AKT activation by a factor of 1.8 compared to non-stimulated cardiac cell constructs. By contrast, the p38 mitogen-activated protein kinase (MAPK), whose activation has been shown to be associated with cardiac cell apoptosis, showed the same activation level as in the control, non-stimulated group.

Effects of long-term magnetic stimulation on metabolic activity and proliferation

The cardiac cell constructs were exposed to an externally generated alternating magnetic field of 10–15 Oe, at a frequency of 5 Hz for 5 days, while control constructs were cultivated without magnetic stimulation. After 5 d of stimulation, the magnetic field was turned off, and both “stimulated” and “non-stimulated” constructs were cultivated for additional 7 d under no field conditions (Figure 3(A)). The constructs were analyzed for metabolic activity, contractile protein expression as well as cell morphology and organization, on day 8 (immediately upon turning off the magnetic stimulation) and 7 d later (day 15 of cultivation) as compared to day 3 of cultivation before stimulation.

The results of metabolic activity of the cardiac cell constructs are presented as the metabolic activity per cell (i.e., normalized to DNA content in the construct relative to day 3, before

magnetic stimulation) (Figure 3(B)). As seen, the metabolic activity per cell was significantly elevated in the cardiac cell constructs exposed to magnetic stimulation for 5 days compared to the control non-stimulated constructs, and further increased from day 8 to day 15 after turning off the magnetic field.

To examine whether the increase in metabolic activity per cell in the magnetically-stimulated cardiac cell constructs was due to cell proliferation, we quantified the expression, by western blot, of the proliferative cell nuclear antigen (PCNA) and vimentin, a non-myocyte cell marker indicative of the CF's number in culture. The quantitative results of both PCNA and vimentin show no significant difference in the expression of these markers in the constructs under magnetic stimulation compared to constructs with no field applied (Figure 4). In both constructs, the PCNA expression on day 8 was elevated compared to its level on day 3, prior to stimulation, after which its level decreased to its initial levels before stimulation. The vimentin level in the magnetic-stimulated and non-stimulated constructs increased constantly over the course of the experiment showing a nearly 3-fold increase in its level at day 15 compared to day 3, indicative of CF proliferation in both constructs.

Collectively, these results indicate that the increase in metabolic activity per cell in the magnetically-stimulated cardiac cell constructs compared to non-stimulated constructs is possibly related to other cell processes rather than cell proliferation per se.

Effects of magnetic stimulation on cardiac cell morphology and organization

Cardiac cell morphology and organization within the MNP-impregnated scaffolds, with or without applying an external magnetic field, were tracked by immunostaining the cardiac cell constructs from days 8 and 15 with antibodies against the contractile protein α-sarcomeric actinin (green) in cardiomyocytes, and f-actin (red), found in both myocyte and non-myocytes. Figure 5 reveals the characteristic cardiac fiber morphology with a massive striation in both stimulated and non-stimulated MNP-scaffolds already on day 8 of cultivation. In both constructs, the non-myocyte cells (stained only in red), formed a well spread, sheet-like supportive layer upon which the cardiomyocyte fibers (stained in green and red) were seen to align.

In lower magnification pictures of day-15 constructs, the magnetic-stimulated constructs show a greater extent of striated fibers compared to the non-stimulated constructs, and the fibers appear to be aligned and anisotropically organized.

Effects of magnetic stimulation on protein expression by western blotting

To further substantiate the differences in tissue quality obtained for different cardiac cell constructs, with or without magnetic stimulation, the expression of the contractile protein Troponin-T representing myocyte cells was quantified by western blotting (Figure 6(A)). The results of day 8 reveal a trend of better preservation of the troponin-T level in the magnetically stimulated constructs compared to the control (non-stimulated) scaffolds. On day 15, this difference reaches a statistical significance, as the level of troponin-T in the magnetically-stimulated constructs increases 2-fold compared to day 8 constructs, while its level in the non-stimulated constructs is decreasing. This observation is in good agreement

with confocal microscope results showing greater extent of myocardial tissue formation in the magnetic-stimulated constructs on day 15 of cultivation (Figure 4).

The expression levels of Connexin-43, a gap-junction protein, expressed both in myocyte and non-myocyte cells, show a trend of higher expression levels in the magnetically stimulated scaffolds compared to nonstimulated constructs.

Discussion

Our study demonstrates that magnetic stimulation of cardiac cells seeded in magnetically-responsive scaffolds promotes myocardial tissue regeneration. The tissue obtained *in vitro* was characterized by a massive striation and aligned cardiac fibers, with greater expression of the contractile protein Troponin-T and Connexin-43, a major protein involved in electrical cellular connections in cardiac tissues. In non-stimulated constructs, these features were less expressed and decayed with cultivation time. Thus, it appears that magnetic stimulation promotes cardiac tissue regeneration and preservation of tissue characteristics in prolonged cultures.

The magnetically-responsive scaffolds were obtained by blending magnetic nanoparticles (MNPs) with alginate solution, calcium crosslinking of the alginate chains and then freeze-drying to create macroporous scaffolds. The inclusion of MNPs did not affect the macro-porous structure or pore size of the scaffold; but did affect the surface topography, as judged by SEM micrographs, showing a rough, grainy surface as compared to the smooth surface of alginate scaffolds with no MNP inclusion (Sapir et al., 2012). Cell adhesion and spreading, mediated *via* cell interactions with HBP/RGD peptides covalently bound to alginate, were also demonstrated within the MNP-impregnated scaffolds. Within 1 h post cell seeding, the confocal microscope micrograph showed cell attachment and initiation of the cell spreading, phenomena that became more evident after 24 h, with the attaining of full cell spreading on the matrix, and cells interacting with each other. These results are in a good agreement with results from numerous studies in 2D cell cultures, which showed that microscale topography can attribute to cellular adherence and spreading (Nikkhah et al., 2012, Pan et al., 2012, Kim et al., 2010).

External magnetic stimulation (5Hz alternating field) of cardiac cells seeded within MNP-impregnated scaffolds, even for a short 20 min period, activated the AKT pathway, a cascade mechanism reported to be a strong promoter of cardiac cell hypertrophy and survival (Cardone et al., 1998, Biggs et al., 1999, Brunet et al., 1999). By contrast, the p38 signaling pathway, a cascade leading to apoptosis and cell death (Wada and Penninger, 2004, Ma et al., 1999), was not affected by the magnetic field and remained unchanged when compared to a control, non-stimulated group. Taken together these results imply that the magnetic field applied to the cardiac cell constructs has a clear immediate effect inducing tissue survival and regeneration.

Long-term magnetic stimulation (5 d) resulted in 3-fold greater metabolic activity per cell in the stimulated vs. non-stimulated constructs. Since there were no differences in the expression levels between the stimulated and non-stimulated constructs of PCNA (a marker

for cell proliferation) or vimentin (indicative for CF's number), the increase in metabolic activity per cell is related to other possible processes, such as cell hypertrophy and organization into a tissue and not due to differences in cell proliferation.

Indeed, the cardiac tissue developed in the magnetically stimulated MNP-scaffolds presented the best features of a functional cardiac muscle tissue, as judged by both the confocal microscope micrographs of the immunostained constructs and their protein expression profiles by western blotting. The 15-day cardiac cell construct subjected to magnetic stimulation revealed a greater extent of striated cardiac fibers compared to non-stimulated constructs and the fibers appear to be aligned. Furthermore, western blot analysis showed that the contractile protein Troponin-T and the gap junction protein Connexin-43 were better preserved in the stimulated 8-day construct and their levels were much greater in the 15-day stimulated constructs compared to the non-stimulated constructs.

The outcomes of this study corroborate our previous findings where we showed that magnetic stimulation promotes the organization of endothelial cells into loop-like structures within MNP-impregnated scaffolds (Sapir et al., 2012). Together, they both suggest mechanostimulation as the possible effect mechanism. Since the MNPs incorporated within the scaffold wall create an anisotropic surface morphology under application of an alternating magnetic field, they magnetize and may induce local scaffold deformation. Deformation like this would apply direct forces of a certain frequency on the cells adhered on the scaffold wall and result in their magneto-mechanical stimulation. This assumption is in a good agreement with our results showing that AKT pathway was activated in magnetically stimulated cell constructs was also shown to be activated by other mechanical stimulations in various experimental systems (Zhang et al., 2011b, Yano et al., 2006, Kippenberger et al., 2005). Nevertheless the precise effect that magnetic field stimulation has on cardiac cells within the magnetically responsive scaffold needs further investigation.

Conclusions

The fundamental goal of cardiac tissue engineering is to heal the heart muscle by replacing the damaged tissue with an engineered tissue graft capable of re-establishing the normal contractile function of the heart. The macroporous magnetically responsive alginate scaffolds described in this paper provide a unique opportunity to non-invasively control the microenvironment of the cardiomyocytes at the cellular scale upon application of a magnetic field, and was shown to generate appropriate physical cues for functional assembly of cardiac cells into functional myocardial tissue. The results of this work as well as of our recent work on endothelial cells demonstrate that magnetic alginate scaffolds exposed to an alternating magnetic field create stimulating microenvironments for engineering functional tissues. The uniqueness of magnetically actuated scaffolds stems from their ability to non-invasively apply a means of mechanical stimulation. This ability is of particular interest for applications *in vivo* where physical stimulus can be also applied to enhance integration of the tissue graft with the host vasculature after transplantation.

In order to accelerate the integration of cardiac patch after implantation, the future studies will be focused on tri-cell culture (cardiomyocytes, cardio-fibroblasts and endothelial cells)

within the magnetic scaffold and optimization of stimulation protocol for inducing the formation of vascularized cardiac patch.

Acknowledgments

Yulia Sapir gratefully acknowledges the Azrieli Foundation for awarding the Azrieli Fellowship supporting her PhD program. The study was partially supported by The Louis and Bessie Stein Family foundation through the Drexel University College of Medicine (BP, YS, SC), American Associates of the Ben-Gurion University of the Negev, Israel (YS), and the National Heart, Lung and Blood Institute (Award Number R01HL107771) (BP). The content is solely the responsibility of the authors and does not necessarily represent the official views of the National Heart, Lung and Blood Institute or the National Institutes of Health. We thank Yang Gao for her help in acquiring SEM images. The scanning electron microscopy was conducted at the Centralized Research Facilities at Drexel University.

Prof. Cohen holds the Claire and Harold Oshry Professor Chair in Biotechnology.

References

BARASH Y, DVIR T, TANDEITNIK P, RUVINOV E, GUTERMAN H, COHEN S. Electric field stimulation integrated into perfusion bioreactor for cardiac tissue engineering. Tissue Eng Part C Methods. 2010; 16:1417–26. [PubMed: 20367291]

BIGGS WH 3RD, MEISENHELDER J, HUNTER T, CAVENEE WK, ARDEN KC. Protein kinase B/Akt-mediated phosphorylation promotes nuclear exclusion of the winged helix transcription factor FKHR1. Proc Natl Acad Sci U S A. 1999; 96:7421–6. [PubMed: 10377430]

BRUNET A, BONNI A, ZIGMOND MJ, LIN MZ, JUO P, HU LS, ANDERSON MJ, ARDEN KC, BLENIS J, GREENBERG ME. Akt promotes cell survival by phosphorylating and inhibiting a Forkhead transcription factor. Cell. 1999; 96:857–68. [PubMed: 10102273]

CARDONE MH, ROY N, STENNICKE HR, SALVESEN GS, FRANKE TF, STANBRIDGE E, FRISCH S, REED JC. Regulation of cell death protease caspase-9 by phosphorylation. Science. 1998; 282:1318–21. [PubMed: 9812896]

CHEN AH, GORTLER DS, KILARU S, ARAIM O, FRANGOS SG, SUMPIO BE. Cyclic strain activates the pro-survival Akt protein kinase in bovine aortic smooth muscle cells. Surgery. 2001; 130:378–81. [PubMed: 11490374]

CHORNY M, POLYAK B, ALFERIEV IS, WALSH K, FRIEDMAN G, LEVY RJ. Magnetically driven plasmid DNA delivery with biodegradable polymeric nanoparticles. FASEB J. 2007; 21:2510–9. [PubMed: 17403937]

DAR A, SHACHAR M, LEOR J, COHEN S. Optimization of cardiac cell seeding and distribution in 3D porous alginate scaffolds. Biotechnol Bioeng. 2002; 80:305–12. [PubMed: 12226863]

DVIR T, KEDEM A, RUVINOV E, LEVY O, FREEMAN I, LANDA N, HOLBOVA R, FEINBERG MS, DROR S, ETZION Y, LEOR J, COHEN S. Prevascularization of cardiac patch on the omentum improves its therapeutic outcome. Proc Natl Acad Sci U S A. 2009; 106:14990–5. [PubMed: 19706385]

DVIR T, LEVY O, SHACHAR M, GRANOT Y, COHEN S. Activation of the ERK1/2 cascade via pulsatile interstitial fluid flow promotes cardiac tissue assembly. Tissue Eng. 2007; 13:2185–93. [PubMed: 17518740]

DVIR T, TIMKO BP, BRIGHAM MD, NAIK SR, KARAJANAGI SS, LEVY O, JIN H, PARKER KK, LANGER R, KOHANE DS. Nanowired three-dimensional cardiac patches. Nat Nanotechnol. 2011; 6:720–5. [PubMed: 21946708]

EDELMAN ER, BROWN L, KOST J, TAYLOR J, LANGER R. Modulated release from polymeric drug delivery systems using oscillating magnetic fields: in vitro and in vivo characteristics. Trans Am Soc Artif Intern Organs. 1984; 30:445–9. [PubMed: 6533921]

FIELDS RD, LANCASTER MV. Dual-attribute continuous monitoring of cell proliferation/cytotoxicity. Am Biotechnol Lab. 1993; 11:48–50.

GERECHT-NIR S, RADISIC M, PARK H, CANNIZZARO C, BOUBLIK J, LANGER R, VUNJAK-NOVAKOVIC G. Biophysical regulation during cardiac development and application to tissue engineering. Int J Dev Biol. 2006; 50:233–43. [PubMed: 16479491]

HEIDI AU HT, CUI B, CHU ZE, VERES T, RADISIC M. Cell culture chips for simultaneous application of topographical and electrical cues enhance phenotype of cardiomyocytes. Lab Chip. 2009; 9:564–75. [PubMed: 19190792]

HORAK D, BABIC M, MACKOVA H, BENES MJ. Preparation and properties of magnetic nano- and microsized particles for biological and environmental separations. J Sep Sci. 2007; 30:1751–72. [PubMed: 17623453]

JOHNSON B, TOLAND B, CHOKSHI R, MOCHALIN V, KOUTZAKI S, POLYAK B. Magnetically responsive paclitaxel-loaded biodegradable nanoparticles for treatment of vascular disease: preparation, characterization and in vitro evaluation of anti-proliferative potential. Curr Drug Deliv. 7:263–73.

KIM DH, LIPKE EA, KIM P, CHEONG R, THOMPSON S, DELANNOY M, SUH KY, TUNG L, LEVCHENKO A. Nanoscale cues regulate the structure and function of macroscopic cardiac tissue constructs. Proc Natl Acad Sci U S A. 2010; 107:565–70. [PubMed: 20018748]

KIPPENBERGER S, LOITSCH S, GUSCHEL M, MULLER J, KNIES Y, KAUFMANN R, BERND A. Mechanical stretch stimulates protein kinase B/Akt phosphorylation in epidermal cells via angiotensin II type 1 receptor and epidermal growth factor receptor. J Biol Chem. 2005; 280:3060–7. [PubMed: 15545271]

LIU TY, HU SH, LIU DM, CHEN SY. Magnetic-sensitive behavior of intelligent ferrogels for controlled release of drug. Langmuir. 2006; 22:5974–8. [PubMed: 16800645]

MA XL, KUMAR S, GAO F, LOUDEN CS, LOPEZ BL, CHRISTOPHER TA, WANG C, LEE JC, FEUERSTEIN GZ, YUE TL. Inhibition of p38 mitogen-activated protein kinase decreases cardiomyocyte apoptosis and improves cardiac function after myocardial ischemia and reperfusion. Circulation. 1999; 99:1685–91. [PubMed: 10190877]

MACDONALD C, FRIEDMAN G, ALAMIA J, BARBEE K, POLYAK B. Time-varied magnetic field enhances transport of magnetic nanoparticles in viscous gel. Nanomedicine (Lond). 2010; 5:65–76. [PubMed: 20025465]

MASSART R. Preparation of Aqueous Magnetic Liquids in Alkaline and Acidic Media. Ieee Transactions on Magnetics. 1981; 17:1247–1248.

NIKKHAH M, EDALAT F, MANOUCHERI S, KHADEMHOSSEINI A. Engineering microscale topographies to control the cell-substrate interface. Biomaterials. 2012; 33:5230–46. [PubMed: 22521491]

ORLOVA Y, MAGOME N, LIU L, CHEN Y, AGLADZE K. Electrospun nanofibers as a tool for architecture control in engineered cardiac tissue. Biomaterials. 2011; 32:5615–24. [PubMed: 21600646]

PAN HA, HUNG YC, SUI YP, HUANG GS. Topographic control of the growth and function of cardiomyoblast H9c2 cells using nanodot arrays. Biomaterials. 2012; 33:20–8. [PubMed: 21982297]

RADISIC M, PARK H, SHING H, CONSI T, SCHOEN FJ, LANGER R, FREED LE, VUNJAK-NOVAKOVIC G. Functional assembly of engineered myocardium by electrical stimulation of cardiac myocytes cultured on scaffolds. Proc Natl Acad Sci U S A. 2004; 101:18129–34. [PubMed: 15604141]

RUVINOV, E., SAPIR, Y., COHEN, S. Cardiac Tissue Engineering. Principles, Materials and Applications. Morgan & Claypool; 2012.

SAPIR Y, COHEN S, FRIEDMAN G, POLYAK B. The promotion of in vitro vessel-like organization of endothelial cells in magnetically responsive alginate scaffolds. Biomaterials. 2012; 33:4100–9. [PubMed: 22417620]

SAPIR Y, KRYUKOV O, COHEN S. Integration of multiple cell-matrix interactions into alginate scaffolds for promoting cardiac tissue regeneration. Biomaterials. 2011; 32:1838–1847. [PubMed: 21112626]

SHACHAR M, BENISHTI N, COHEN S. Effects of mechanical stimulation induced by compression and medium perfusion on cardiac tissue engineering. Biotechnol Prog. 2012; 28:1551–9. [PubMed: 22961835]

SHACHAR M, TSUR-GANG O, DVIR T, LEOR J, COHEN S. The effect of immobilized RGD peptide in alginate scaffolds on cardiac tissue engineering. Acta Biomater.

SHACHAR M, TSUR-GANG O, DVIR T, LEOR J, COHEN S. The effect of immobilized RGD peptide in alginate scaffolds on cardiac tissue engineering. Acta Biomater. 2011; 7:152–62. [PubMed: 20688198]

SHAPIRO L, COHEN S. Novel alginate sponges for cell culture and transplantation. Biomaterials. 1997; 18:583–90. [PubMed: 9134157]

SINGER VL, JONES LJ, YUE ST, HAUGLAND RP. Characterization of PicoGreen reagent and development of a fluorescence-based solution assay for double-stranded DNA quantitation. Anal Biochem. 1997; 249:228–38. [PubMed: 9212875]

TAKAHASHI T, TANIGUCHI T, KONISHI H, KIKKAWA U, ISHIKAWA Y, YOKOYAMA M. Activation of Akt/protein kinase B after stimulation with angiotensin II in vascular smooth muscle cells. Am J Physiol. 1999; 276:H1927–34. [PubMed: 10362672]

WADA T, PENNINGER JM. Mitogen-activated protein kinases in apoptosis regulation. Oncogene. 2004; 23:2838–49. [PubMed: 15077147]

YANO S, KOMINE M, FUJIMOTO M, OKOCHI H, TAMAKI K. Activation of Akt by mechanical stretching in human epidermal keratinocytes. Exp Dermatol. 2006; 15:356–61. [PubMed: 16630075]

YOU JO, RAFAT M, YE GJ, AUGUSTE DT. Nanoengineering the heart: conductive scaffolds enhance connexin 43 expression. Nano Lett. 2011; 11:3643–8. [PubMed: 21800912]

ZHANG B, XIAO Y, HSIEH A, THAVANDIRAN N, RADISIC M. Micro- and nanotechnology in cardiovascular tissue engineering. Nanotechnology. 2011a; 22:494003. [PubMed: 22101261]

ZHANG BC, ZHOU ZW, LI XK, XU YW. PI-3K/AKT signal pathway modulates vascular smooth muscle cells migration under cyclic mechanical strain. Vasa. 2011b; 40:109–16. [PubMed: 21500175]

ZHAO X, KIM J, CEZAR CA, HUEBSCH N, LEE K, BOUHADIR K, MOONEY DJ. Active scaffolds for on-demand drug and cell delivery. Proc Natl Acad Sci U S A. 108:67–72.

ZIMMERMANN WH, FINK C, KRALISCH D, REMMERS U, WEIL J, ESCHENHAGEN T. Three-dimensional engineered heart tissue from neonatal rat cardiac myocytes. Biotechnol Bioeng. 2000; 68:106–14. [PubMed: 10699878]

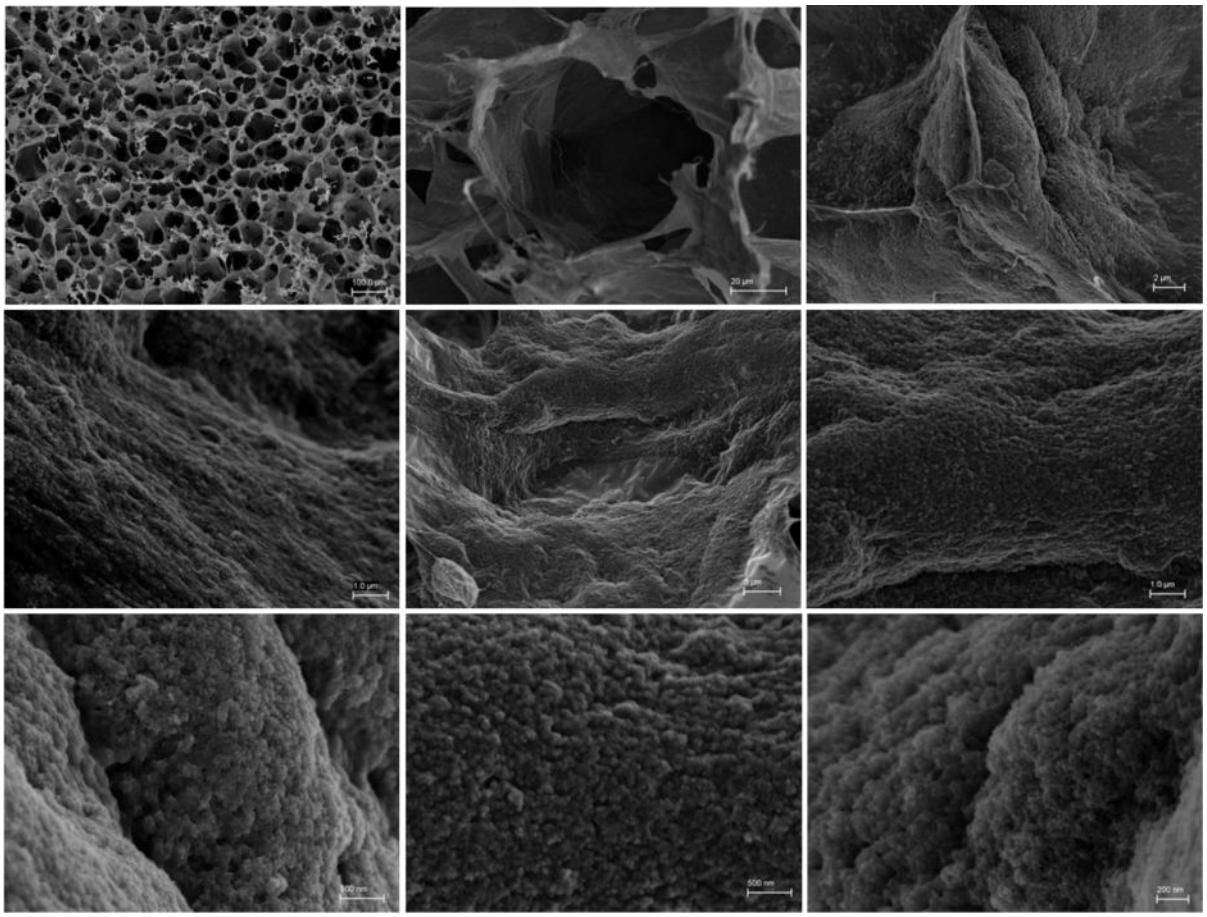

Figure 1.
Overall scaffold and surface morphology: Scanning electron microscopy (SEM) images of the MNP-impregnated scaffold.

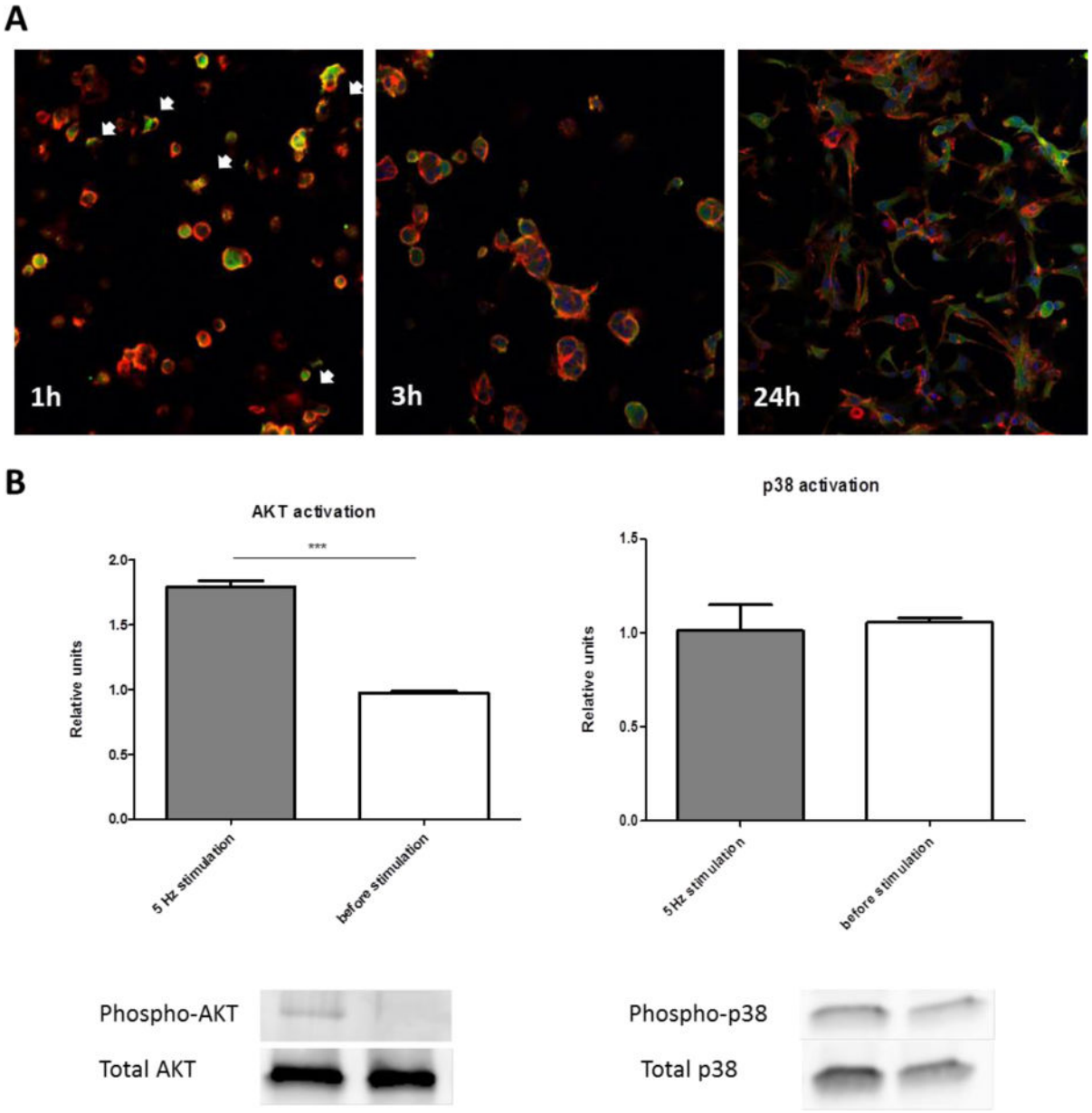

Figure 2.

Cardiac cells adhesion onto the macroporous MNP-impregnated scaffolds. **(A)** Immunostaining for vinculin (green), F-actin (red) and nuclei (blue), 1, 3 and 24 h post-seeding. Magnification is ×20. AKT **(B)** and P38 **(C)** phosphorylation by western blot analyses on day 3 post-seeding. Levels of phosphorylation are presented as fold increase in band density over non-stimulated cell constructs and correspond to the mean ± SEM of two independent experiments. All results are normalized by a control group (without stimulation). Asterisks denote significant differences (by T-test) *$p < 0.05$, **$p < 0.01$ and ***$p < 0.005$).

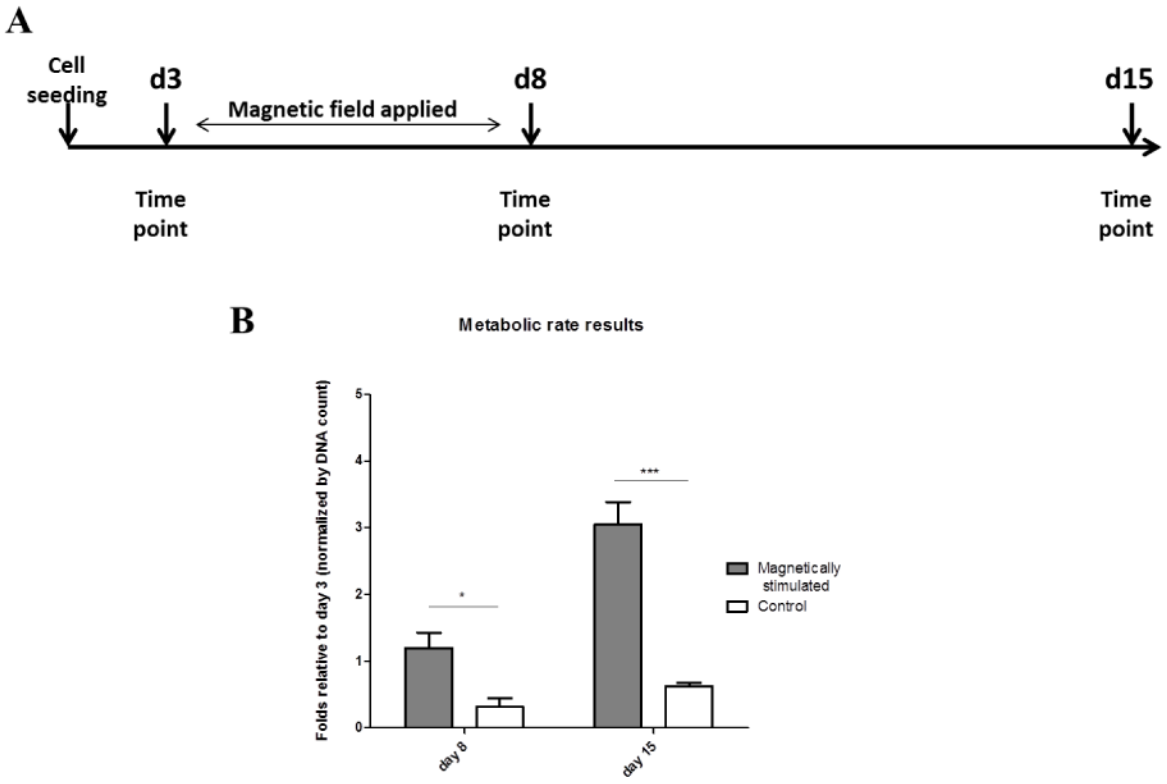

Figure 3.

(A) Experimental time scale. (B) Metabolic activity per cell in the different constructs. Data (n= 3–5 constructs per tested group) presented are normalized to the DNA content in the construct, relative to day 3 respectively. Asterisks denote significant difference (by two-way ANOVA) *$p < 0.05$, **$p < 0.01$ and ***$p < 0.005$ (Bonferroni's pos-hoc test was used for comparison between the groups).

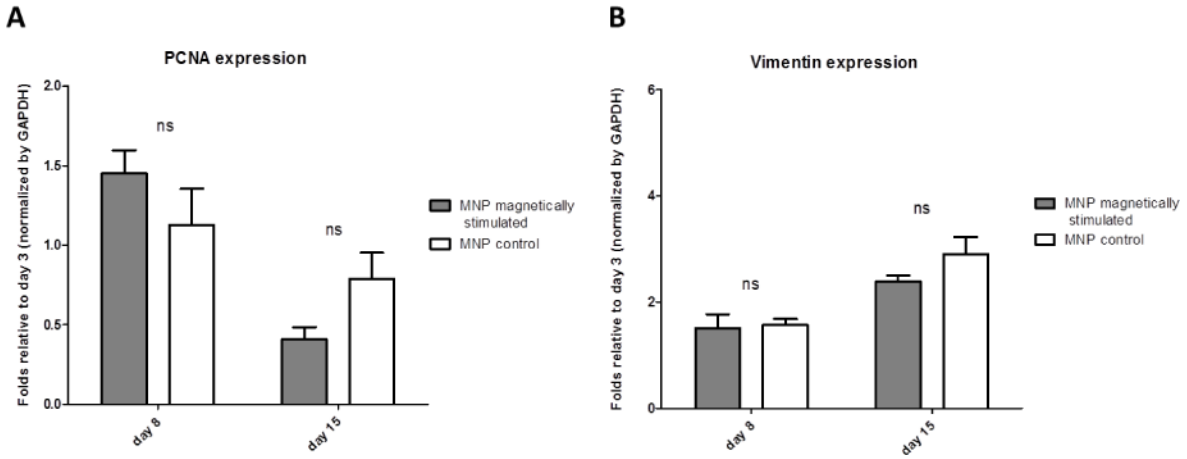

Figure 4.

Expression of non-myocyte cell proteins by Western blots. Protein expression is presented as relative to day 3 before stimulation, for (A) PCNA, (B) vimentin. Asterisks denote significant difference (by 2-way ANOVA), *$p < 0.05$, **$p < 0.01$ and ***$p < 0.005$ (Bonferroni's pos-hoc test was used for comparison between the groups), ns represents non-significant difference.

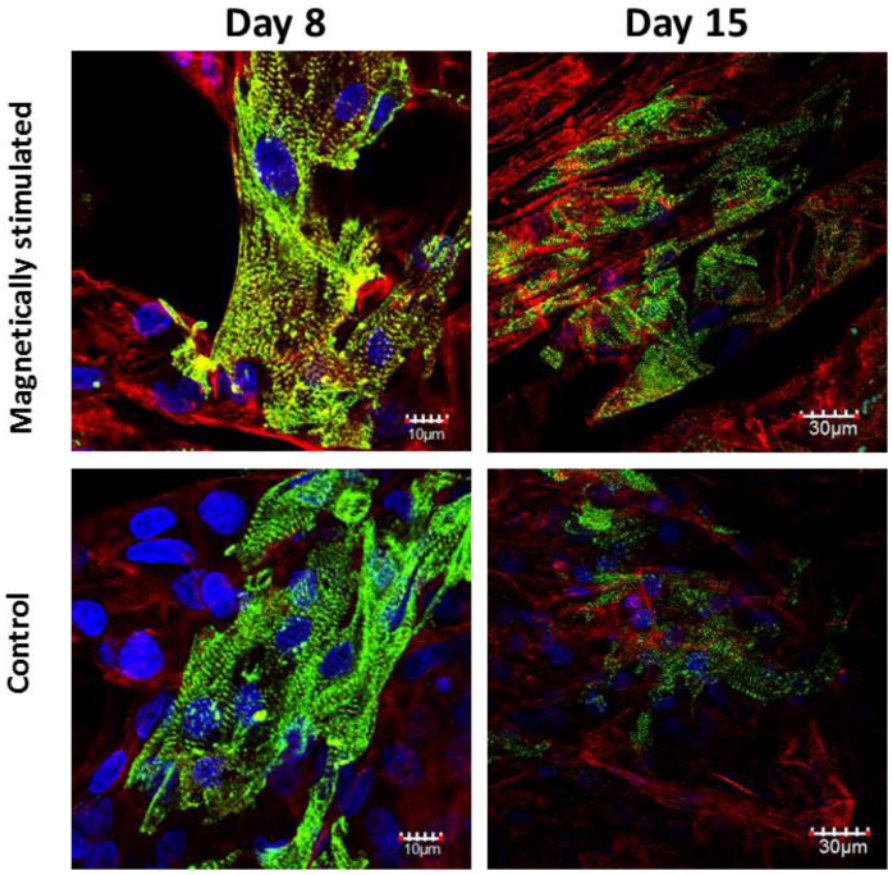

Figure 5.

Cardiac cell organization within MNP impregnated constructs, on day 8 and day15 post cell seeding. The cells were stained for alpha-actinin (green), F-actin (red) and nuclei (blue).

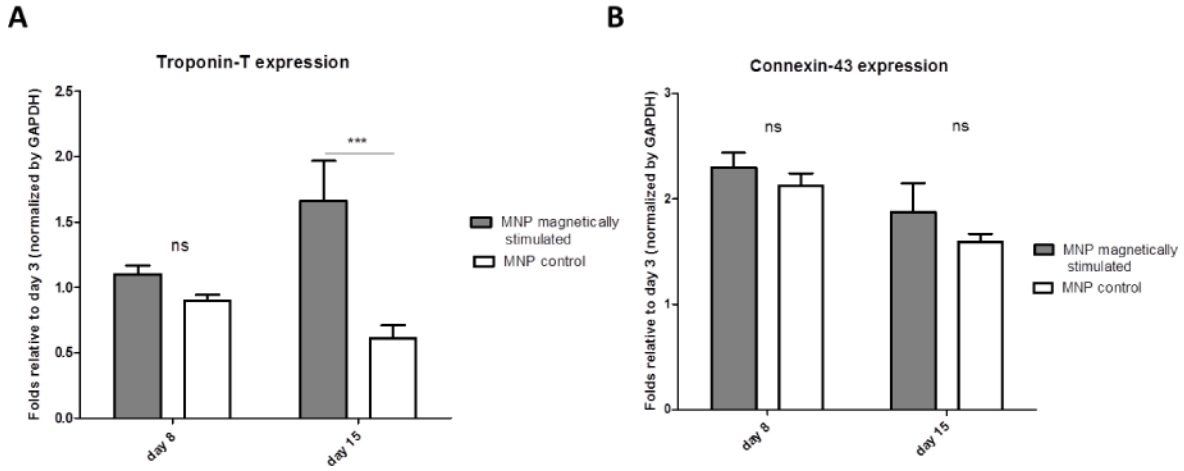

Figure 6.

Expression of representative cardiac cell markers by Western blots. Protein expression is presented as relative to day 3 before stimulation, for **(A)** cardiac Troponin T, **(B)** Connexin-43. Asterisks denote significant difference (by 2-way ANOVA), *$p < 0.05$, **$p < 0.01$ and ***$p < 0.005$ (Bonferroni's pos-hoc test was used for comparison between the groups), ns represents non-significant difference.